Article

Self-Assembly and Luminescence of Oligo(*p*-phenylene vinylene) Amphiphiles

James F. Hulvat, Marina Sofos, Keisuke Tajima, and Samuel I. Stupp

J. Am. Chem. Soc., **2005**, 127 (1), 366-372• DOI: 10.1021/ja047210m • Publication Date (Web): 03 December 2004

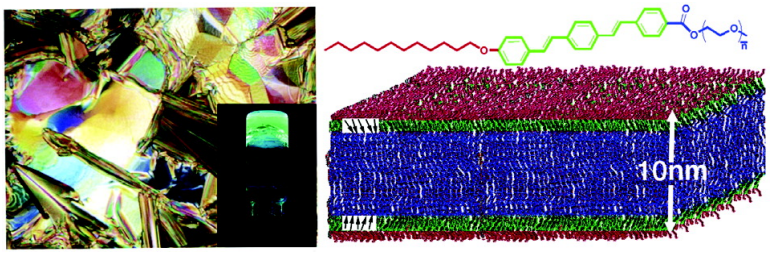

More About This Article

Additional resources and features associated with this article are available within the HTML version:

- Supporting Information
- Links to the 17 articles that cite this article, as of the time of this article download
- Access to high resolution figures
- Links to articles and content related to this article
- Copyright permission to reproduce figures and/or text from this article

View the Full Text HTML

J|A|C|S
ARTICLES
Published on Web 12/03/2004

Self-Assembly and Luminescence of Oligo(*p*-phenylene vinylene) Amphiphiles

James F. Hulvat,[†] Marina Sofos,[†] Keisuke Tajima,[†] and Samuel I. Stupp*[,†,‡,§]

Contribution from the Department of Materials Science and Engineering, Department of Chemistry, and Feinberg School of Medicine, Northwestern University, Evanston, Illinois 60208

Received May 12, 2004; E-mail: s-stupp@northwestern.edu

Abstract: We have synthesized a series of amphiphilic molecules consisting of oligo(phenylene vinylene) (OPV) asymmetrically end-substituted with a hydrophilic poly(ethylene glycol) (PEG) segment and a hydrophobic alkyl chain. This amphiphilic structure induces self-assembly into both thermotropic and lyotropic lamellar liquid crystalline (LC) phases. The molecules form strongly fluorescent, self-supporting gels in both water and polar organic solvents, even at high concentrations on the order of 30 wt %. These self-assembled structures have been characterized by small-angle X-ray scattering (SAXS), differential scanning calorimetry (DSC), and polarized optical microscopy (POM). Photoluminescence (PL) is influenced by the structure of the material, with enhanced emission in the LC state due to assembly of the chromophore in confined two-dimensional layers. Self-assembly controlling molecular aggregation at the nanoscale could significantly improve the performance of OPV-based materials in optoelectronic devices.

Introduction

Previous research efforts have led to the synthesis of many conjugated polymers, particularly derivatives of poly(phenylene vinylene) (PPV), soluble in organic solvents and easily processed into films with great promise as organic electronic materials.[1−4] Controlling the nanoscale structure of rodlike conjugated polymers has proven difficult. However, supramolecular order plays a critical role in device performance, as both charge mobility and luminescent efficiency are influenced by molecular aggregation and structural defects.[5,6] π-Conjugated oligomers, first investigated as model compounds for conjugated polymers, are now widely studied for use in optoelectronic devices because their well-defined chemical structure facilitates tuning of electronic properties.[7−9] Use of well-defined oligomers reduces defect density while enabling more control over the effective conjugation length. In particular, oligo(*p*-phenylene vinylene)s (OPVs) are being investigated for use in solar cells and light-emitting diodes (LEDs) due to their stability, high luminescent efficiency, and ease of synthesis.[10,11] OPVs with solubilizing substituents combine the low-cost, solution-based processing of conjugated polymers with the improved structural control inherent to oligomers.[6,9,11,12]

One approach to control nanoscale structure in conjugated polymers has been to design molecules that could exhibit thermotropic or lyotropic liquid crystalline (LC) behavior.[4,13] Among these are the "hairy-rod"-type liquid crystalline polymers

[†] Department of Materials Science and Engineering.
[‡] Department of Chemistry.
[§] Feinberg School of Medicine.

(1) (a) Akcelrud, L. *Prog. Polym. Sci.* **2003**, *28*, 875−962. (b) Babudri, F.; Cicco, S. R.; Farinola, G. M.; Naso, F.; Bolognesi, A.; Porzio, W. *Macromol. Rapid Commun.* **1996**, *17*, 905−911. (c) Bianchi, C.; Cecchetto, E.; Francois, B. *Synth. Met.* **1999**, *102*, 916−917.
(2) Grell, M.; Bradley, D. D. C. *Adv. Mater.* **1999**, *11*, 895−905.
(3) Hwang, D. H.; Shim, H. K. *Thin Solid Films* **2002**, *417*, 166−170.
(4) Egbe, D. A. M.; Roll, C. P.; Klemm, E. *Des. Monomers Polym.* **2002**, *5*, 245−275.
(5) (a) Schwartz, B. J. *Annu. Rev. Phys. Chem.* **2003**, *54*, 141−172. (b) McQuade, D. T.; Kim, J.; Swager, T. M. *J. Am. Chem. Soc.* **2000**, *122*, 5885−5886. (c) Kim, J.; Levitsky, I. A.; McQuade, D. T.; Swager, T. M. *J. Am. Chem. Soc.* **2002**, *124*, 7710−7718. (d) Cheng, H. L.; Lin, K. F. *J. Polym. Res. (Taiwan)* **1999**, *6*, 123−131. (e) Schenning, A. P. H. J.; Peeters, E.; Meijer, E. W. *J. Am. Chem. Soc.* **2000**, *122*, 4489−4495. (f) Chang, W. P.; Whang, W. T. *Polymer* **1996**, *37*, 3493−3499. (g) Herz, L. M.; Daniel, C.; Silva, C.; Hoeben, F. J. M.; Schenning, A. P. H. J.; Meijer, E. W.; Friend, R. H.; Phillips, R. T. *Phys. Rev. B* **2003**, *68*, 045203. (h) Gin, D.; Yonezawa, K. *Synth. Met.* **2001**, *121*, 1291−1294. (i) Fritz, K. P.; Scholes, G. D. *J. Phys. Chem. B* **2003**, *107*, 10141−10147. (j) Cacialli, F.; Feast, W. J.; Friend, R. H.; de Jong, M.; Lovenich, P. W.; Salaneck, W. R. *Polymer* **2002**, *43*, 3555−3561. (k) Cacialli, F.; Friend, R. H.; Feast, W. J.; Lovenich, P. W. *Chem. Commun.* **2001**, 1778−1779.
(6) (a) Ajayaghosh, A.; George, S. J.; Praveen, V. K. *Angew. Chem., Int. Ed.* **2003**, *42*, 332−335. (b) Schenning, A. P. H. J.; El-ghayoury, A.; Peeters, E.; Meijer, E. W. *Synth. Met.* **2001**, *121*, 1253−1256. (c) Jonkheijm, P. J.; Fransen, M.; Schenning, A. P. H. J.; Meijer, E. W. *J. Chem. Soc., Perkin Trans.* **2001**, *2*, 1280−1286.
(7) (a) Nguyen, T. Q.; Yee, R. Y.; Schwartz, B. J. *J. Photochem. Photobiol., A* **2001**, *144*, 21−30. (b) van Hutten, P. F.; Krasnikov, V. V.; Hadziioannou, G. *Acc. Chem. Res.* **1999**, *32*, 257−265. (c) Gill, R. E.; Hilberer, A.; van Hutten, P. F.; Berentschot, G.; Werts, M. P. L.; Meetsma, A.; Wittmann, J.-C.; Hadzioannou, G. *Synth. Met.* **1997**, *84*, 637−638. (d) Meghdadi, F.; Leising, G.; Fischer, W.; Stelzer, F. *Synth. Met.* **1996**, *76*, 113−115. (e) Swager, T. M.; Gil, C. J.; Wrighton, M. S. *J. Phys. Chem.* **1995**, *99*, 4886−4893. (f) Katz, H. E.; Bent, S. F.; Wilson, W. L.; Schilling, M. L.; Ungashe, S. B. *J. Am. Chem. Soc.* **1994**, *116*, 6631−6635. (g) Schenning, A. P. H. J.; Jonkheijm, P.; Peeters, E.; Meijer, E. W. *J. Am. Chem. Soc.* **2001**, *123*, 409−416.
(8) Geiger, C.; Stanescu, M.; Chen, L. H.; Whitten, D. G. *Langmuir* **1999**, *15*, 2241−2245.
(9) Lowe, C.; Weder, C. *Adv. Mater.* **2002**, *14*, 1625−1629.
(10) (a) Seferos, D. S.; Banach, D. A.; Alcantar, N. A.; Israelachvili, J. N.; Bazan, G. C. *J. Org. Chem.* **2004**, *69*, 1110−1119. (b) Robinson, M. R.; Wang, S. J.; Heeger, A. J.; Bazan, G. C. *Adv. Funct. Mater.* **2001**, *11*, 413−419. (c) Goodson, T.; Li, W.; Gharavi, A.; Yu, L. *Adv. Mater.* **1997**, *9*, 639−643. (d) Gebhardt, V.; Bacher, A.; Thelakkat, M.; Stalmach, U.; Meier, H.; Schmidt, H.-W.; Haarer, D. *Synth. Met.* **1997**, *90*, 123−126. (e) Hudson, A. J.; Tamura, S. I.; Grieve, M. B.; Richardson, T.; Wong, J. E.; Bruce, D. W. *J. Mater. Chem.* **1995**, *5*, 1867−1870. (f) Geens, W.; Portmans, J.; Jain, S. C.; Nijs, J.; Mertens, R.; Veenstra, S. C.; Krasnikov, V. V.; Hadziiaonnou, G. *Sol. Energy Mater. Sol. Cells* **2000**, *61*, 43−51.
(11) Tao, Y.; Donat-Bouillud, A.; D'Iorio, M.; Lam, J.; Gorjanc, T. C.; Py, C.; Wong, M. S.; Li, Z. H. *Thin Solid Films* **2000**, *363*, 298−301.
(12) Era, M.; Koganemaru, J.; Tsutsui, T.; Watakabe, A.; Kunitake, T. *Synth. Met.* **1997**, *91*, 83−85.

10.1021/ja047210m CCC: $30.25

Scheme 1. Synthesis of OPV Amphiphile[a]

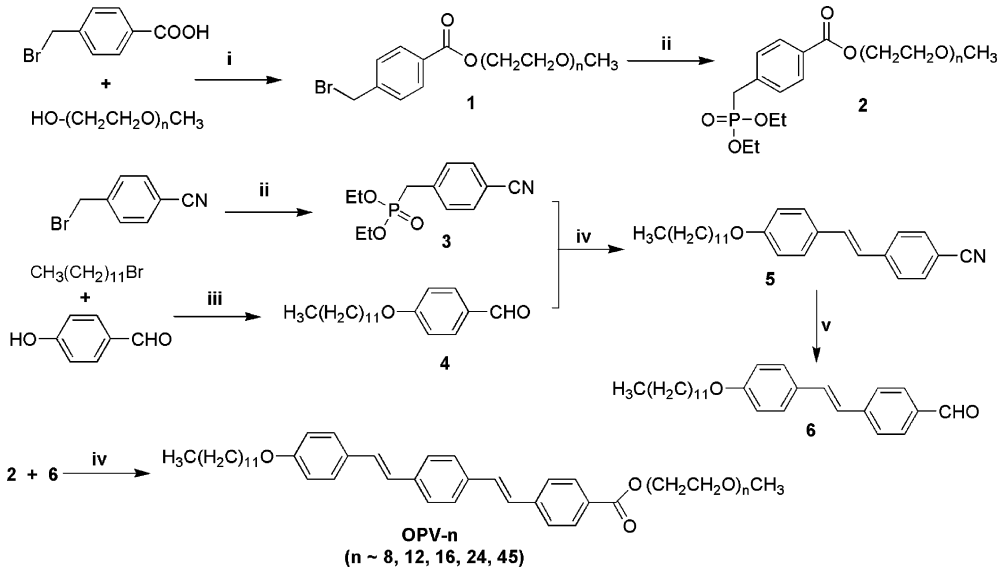

[a] Reaction conditions: (i) DPTS/EDIC, CH_2Cl_2. (ii) $P(OEt)_3$, 130 °C. (iii) K_2CO_3, 18-crown-6, acetone, 56 °C. (iv) LDA, cyclohexane/THF, −78 °C. (v) DIBAL-H, Et_2O, 0 °C.

(LCPs), in which flexible alkyl side chains added for solubility induce nanophase separation of the rigid, conjugated polymer backbone.[3,14] A more direct approach is to incorporate calamitic mesogens as side chains on a conjugated polymer backbone.[15,16] Both methods can result in layered, smectic ordering of the polymer, but only micron-sized domains are generally obtained due to the viscosity and rigidity of the polymer's extended backbone conjugation, which inhibits formation of the large monodomains needed in device applications.[2,16]

Use of conjugated, liquid crystalline oligomers can improve ordering, and several LC oligomers based on substituted OPV rods have been reported.[17] Many are analogues of conjugated LCPs, with flexible alkyl chains grafted laterally onto the molecule.[6,18] However, this introduces bulky, sterically hindering groups that disrupt coplanarity within the π-conjugated system.[19] End-substitution is preferred for this reason; however, there are few reports of end-substituted OPVs that form LC phases.[20] Typically, these are symmetrically substituted to simplify their synthesis. While asymmetric substitution can improve ordering of OPV mesogens, only a few examples of truly amphiphilic, asymmetrically end-substituted OPVs have been reported, and their mesophase behavior has not been extensively characterized.[8,19,21]

We report here the synthesis and characterization of a novel series of amphiphiles consisting of a well-defined OPV trimer asymmetrically end-substituted with a hydrophobic alkyl chain and a hydrophilic poly(ethylene glycol) (PEG). These molecules form lyotropic and thermotropic LC phases in polar solvents, and we can tune the solubility and mesophase structure by controlling the length of the PEG block. With a sufficiently long PEG, OPV amphiphiles become water soluble, a significant advantage for large-scale processing of materials. Though a number of water-soluble PPV polymers have been reported,[22] only a few examples of water-soluble OPVs have been reported, and these were solubilized through the use of ionic substituents.[23] With the nonionic amphiphile reported here, liquid crystallinity is used to control OPV aggregation, influencing exciton mobility, fluorescence, and potentially leading to improved charge carrier mobility in heterojunction solar cells or enabling more efficient, polarized emission from organic light-emitting diodes (OLEDs).

Results and Discussion

Synthesis. The syntheses of OPV amphiphiles are shown in Scheme 1 and described in detail in the Experimental Methods.

(13) (a) Hamaguchi, M.; Yoshino, K. *Jpn. J. Appl. Phys., Part 2* **1994**, *33*, L1689−L1692. (b) Lee, M.; Yoo, Y. S. *J. Mater. Chem.* **2002**, *12*, 2161−2168. (c) Eckert, J.-F.; Maciejczuk, U.; Guillon, D.; Nierengarten, J.-F. *Chem. Commun.* **2001**, 1278−1279.
(14) Li, W. J.; Wang, H. B.; Yu, L. P.; Morkved, T. L.; Jaeger, H. M. *Macromolecules* **1999**, *32*, 3034−3044.
(15) (a) Chen, H. P.; Katsis, D.; Mastrangelo, J. C.; Marshall, K. L.; Chen, S. H.; Mourey, T. H. *Chem. Mater.* **2000**, *12*, 2275−2281. (b) Onoda, M.; Tada, K.; Ozaki, M.; Yoshino, K. *Electron. Eng. Jpn.* **2002**, *138*, 1−8.
(16) Oguma, J.; Dai, X. M.; Akagi, K. *Mol. Cryst. Liq. Cryst.* **2001**, *365*, 1287.
(17) (a) Geng, Y. H.; Chen, A. C. A.; Ou, J. J.; Chen, S. H.; Klubek, K.; Vaeth, K. M.; Tang, C. W. *Chem. Mater.* **2003**, *15*, 4352−4360. (b) Culligan, S. W.; Geng, Y. H.; Chen, S. H.; Klubek, K.; Vaeth, K. M.; Tang, C. W. *Adv. Mater.* **2003**, *15*, 1176−1180. (c) Precup-Blaga, F. S.; Schenning, A. P. H. J.; Meijer, E. W. *Macromolecules* **2003**, *36*, 565−572. (d) Tinh, N. H.; Zann, A.; Dubois, J. C.; Billard, J. *J. Phys.* **1978**, *39*, 1283−1286. (e) Maddux, T.; Li, W. J.; Yu, L. P. *J. Am. Chem. Soc.* **1997**, *119*, 844−845.
(18) Zhu, W.; Li, W. J.; Yu, L. P. *Macromolecules* **1997**, *30*, 6274−6279.
(19) Tao, Y.; Donat-Bouillud, A.; D'Iorio, M.; Lam, J.; Gorjanc, T. C.; Py, C.; Wong, M. S. *Synth. Met.* **2000**, *111*, 417−420.
(20) (a) Davis, R.; Mallia, V. A.; Das, S. *Chem. Mater.* **2003**, *15*, 1057−1063. (b) Wong, M. S.; Samoc, M.; Samoc, A.; Luther-Davies, B.; Humphrey, M. G. *J. Mater. Chem.* **1998**, *8*, 2005−2009. (c) Eckert, J. F.; Nicoud, J.-F.; Guillon, D.; Nierengarten, J.-F. *Tetrahedron Lett.* **2000**, *41*, 6411−6414.
(21) (a) Watakabe, A.; Kunitake, T. *Thin Solid Films* **1990**, *186*, L21−L24. (b) Wang, H. B.; Wang, H. H.; Urban, V. S.; Littrell, K. C.; Thiyagarajan, P.; Yu, L. P. *J. Am. Chem. Soc.* **2000**, *122*, 6855−6861. (c) Wang, H.; You, W.; Jiang, P.; Yu, L.; Wang, H. H. *Chem.−Eur. J.* **2004**, *10*, 986−993.
(22) (a) Peng, Q. G.; Yang, J. L.; He, Q. G.; Bai, F. L. *Synth. Met.* **2003**, *135*, 163−164. (b) Li, H. M.; Xiang, C. H.; Li, Y. L.; Xiao, S. Q.; Fang, H. J.; Zhu, D. B. *Synth. Met.* **2003**, *135*, 483−484. (c) Fujii, A.; Sonoda, T.; Fujisawa, T.; Ootake, R.; Yoshino, K. *Synth. Met.* **2001**, *119*, 189−190. (d) Wang, H. L.; McBranch, D. W.; Donohoe, R. J.; Xu, S.; Kraabel, B.; Chen, L. H.; Whitten, D.; Helgeson, R.; Wudl, F. *Synth. Met.* **2001**, *121*, 1367−1368. (e) Fujii, A.; Sonoda, T.; Yoshino, K. *Jpn. J. Appl. Phys., Part 2* **2000**, *39*, L249−L252. (f) Wang, D. L.; Lal, J.; Moses, D.; Bazan, G. C.; Heeger, A. J. *Chem. Phys. Lett.* **2001**, *348*, 411−415.
(23) (a) Liu, B.; Gaylord, B. S.; Wang, S.; Bazan, G. C. *J. Am. Chem. Soc.* **2003**, *125*, 6705−6714. (b) Gaylord, B. S.; Wang, S. J.; Heeger, A. J.; Bazan, G. C. *J. Am. Chem. Soc.* **2001**, *123*, 6417−6418. (c) Stork, M.; Gaylord, B. S.; Heeger, A. J.; Bazan, G. C. *Adv. Mater.* **2002**, *14*, 361−366. (d) Sun, J. Z.; Sun, J. Q.; Ma, Y. G.; Zhang, X.; Shen, J. C. *Mater. Sci. Eng., C* **1999**, *10*, 83−86.

Table 1. LC Mesophase Transitions Observed for OPV Amphiphiles

OPV-n^a	M_w (g/mol)^b	$M_w/M_n{}^c$	T_m (°C)	T_{LC} (°C)^d	T_c (°C)^e
OPV-8	350	1.01	<rt	122	160
OPV-12	550	1.02	<rt	124	151
OPV-16	750	1.02	30	126, 137	146
OPV-24	1100	1.03	42	109, 120	131
OPV-45	2000	1.02	49	100, 109	123

[a] The *n* is the average number of repeat units in PEG blocks. [b] Average molecular weight of PEG block. [c] Polydispersity of OPV amphiphiles (determined by GPC). [d] Liquid crystalline mesophase transition(s). [e] Clearing temperature of LC phase.

The conjugated vinylene bond was formed using the Horner−Emmons reaction between phosphonate **2** and aldehyde **4** at a low temperature to obtain *trans*-phenylene vinylene **5**.

Aldehyde **6** was obtained by reduction of the cyano group in **5** with diisobutylaluminum hydride. To avoid solubility problems with unsubstituted OPV, we chose the coupling reaction of PEG−phosphonate **2** and aldehyde **6** as the last step. While the lengths of the OPV segment and alkyl tail were kept constant, the PEG block was varied from an average of 8 to 45 repeat units in order to study its effect on mesophase behavior (PEG M_w = 350−2000 g/mol, M_w/M_n = 1.02).

Thermotropic Mesophases. The OPV amphiphiles synthesized were found to be thermotropic LCs, with the mesophase structure highly dependent on the length of the PEG block. Below **OPV-16**, the molecules form liquid crystals at room temperature. As the length of the hydrophilic block increases, the PEG crystallizes and the thermal range of the mesophase narrows. Table 1 summarizes the molecular weight and thermal transitions observed for each amphiphile. Transition temperatures were determined from differential scanning calorimetry (DSC) (scans shown in Supporting Information).

Small-angle X-ray scattering (SAXS) indicates a smectic structure for all the amphiphiles studied. Figure 1 shows small- and wide-angle X-ray diffraction patterns for the OPV amphiphiles, with the interlayer spacing plotted in the inset of Figure 1a as a function of PEG length. The interlayer spacing is approximately equal to the fully extended lengths of the molecules, indicating significant interdigitation and/or tilt within a bilayer smectic structure. The higher-order peaks observed between 2 and 4° 2θ disappear with longer PEG chains, as does the sharp wide-angle peak at 4.3 Å, which is likely to correspond to the breakup of OPV ordering within the smectic layers. Two other peaks appear at 4.6 and 3.8 Å, which may arise from the crystal structure of the PEG block as these peaks were also observed in control PEG-alkyl diblock molecules without OPV. The X-ray data indicate that at room temperature OPV amphiphiles with short PEG chains form an interdigitated bilayer smectic phase with a highly ordered OPV layer. As the length of the hydrophilic segment increases, PEG crystallization disrupts the OPV layer, resulting in a less-ordered structure.

The OPV amphiphiles show distinctive, strongly birefringent mesophase textures when analyzed by polarized optical microscopy (POM). These textures were compared with known ones in the literature;[24,25] however, the similarities among higher-ordered smectic phases and the complexity of the bilayer structure needed further characterization for structural determination. In Figure 2, preliminary phase assignments are proposed for the OPV layer of the LC, based on X-ray and DSC results as well as POM textures.

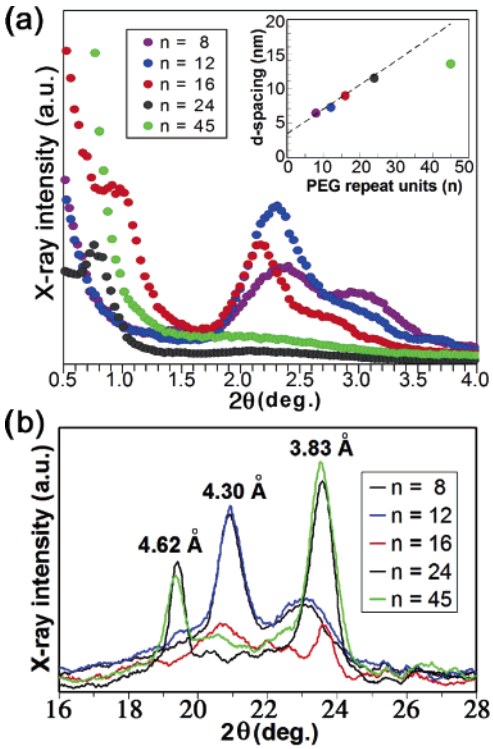

Figure 1. (a) Small-angle X-ray scattering of OPV amphiphiles. Inset shows interlayer spacing as a function of PEG length determined from the first-order diffraction peak. Dashed line is the fully extended length of one molecule. (b) Wide-angle X-ray diffraction of OPV amphiphiles.

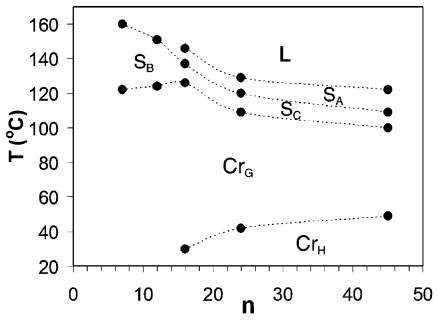

Figure 2. Phase diagram of transitions observed in DSC as a function of PEG length, with preliminary phase assignments.

The competing influence of the OPV and PEG segments on amphiphile aggregation is clear from the phase diagram. A distinct transition occurs above **OPV-12** as the size of the hydrophilic PEG exceeds that of the hydrophobe (M_w = 494 g/mol for the alkyl-OPV). Figure 3 shows a mosaic birefringence texture, similar to that of the smectic B (S_B) mesophase[24] observed for shorter PEG lengths.

Here, S_B ordering is driven by OPV aggregation, while less-ordered smectic C (S_C) and smectic A (S_A) phases result when longer PEG blocks frustrate order within the OPV sublayers. At lower temperatures, a texture similar to that of the crystalline smectic G (Cr_G) mesophase is observed, in which OPV molecules are hexagonally ordered in crystal-like layers with positional and orientational order, but retaining the rotational and diffusional motion of a liquid.[24] In longer OPV amphiphiles at room temperature, crystallization of the hydrophilic PEG

(24) Kumar, S. *Liquid Crystals*; Cambridge University Press: Cambridge, 2001.
(25) Gray, G. W.; Goodby, J. W. G. *Smectic Liquid Crystals: Textures and Structures*; Leonard Hill: London, 1984.

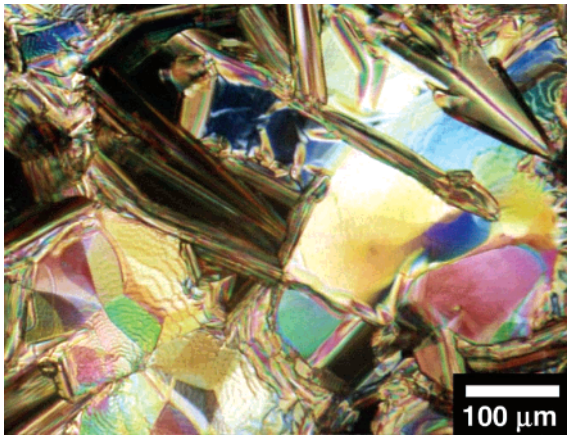

Figure 3. Mosaic birefringence texture of the **OPV-12** amphiphile at 130 °C, observed between crossed polarizers.

Table 2. UV−vis Absorption and Photoluminescence (PL) of OPV Amphiphiles

	λ_{abs} (nm)[a] THF soln	λ_{PL} (nm)[b] THF soln	λ_{abs} (nm)[c] THF film	λ_{PL} (nm)[d] THF film	λ_{PL} (nm)[e] CH_3CN film
OPV-8	375	467	308	510	508
OPV-12	377	467	309	508	507
OPV-16	375	466	320	508	504
OPV-24	376	468	322	506	468
OPV-45	375	468	335	507	467

[a] Absorption in THF solution (375 nm excitation). [b] PL emission maximum in THF solution (375 nm excitation). [c] Absorption in films spin-coated from THF (310 nm excitation). [d] PL emission maximum in films spin-coated from THF (310 nm excitation). [e] PL emission maximum in films spin-coated from CH_3CN (310 nm excitation).

block inhibits molecular rotation, as occurs in the transition from the Cr_G to the Cr_H mesophase. While this transition increases ordering of the hydrophilic sublayer, crystallization of the PEG block may actually disrupt packing in the OPV sublayers, due to differences in the preferred packing arrangement of the two segments. This disruption of the OPV sublayer should be evident in the spectroscopic behavior of the OPV amphiphiles.

Spectroscopic Characterization. The structural characterization of these systems demonstrates how variation in PEG length can change the aggregation state of OPV segments. This should influence the optical and electronic properties of these materials to a greater extent than is possible with standard solution-based processing of OPVs. Thus, UV−vis absorption and photoluminescence (PL) spectroscopy were used to investigate the effect of PEG length on OPV aggregation in solutions and in thin films (Table 2).

Dilute, well-solvated solutions of OPV amphiphiles in tetrahydrofuran (THF) showed absorption and PL emission at 375 and 467 nm, respectively, with no effect of PEG length (Figure 4). However, in spin-coated films, the length of PEG segments had a significant effect on the λ_{abs} of UV absorption. All films showed enhanced vibronic structure and an absorption blue-shift, indicating H-type aggregation with parallel alignment of the OPV transition dipole moments,[26] consistent with a low tilt angle and no interdigitation of the OPV segments within the bilayer smectic structure. This results in two distinct OPV layers (Figure 4c) in which exciton coupling can occur between molecules within a layer, but not between adjacent layers. The longer the PEG block, the smaller the λ_{abs} blue-shift, as

(26) Whitten, D. G. *Acc. Chem. Res.* **1993**, *26*, 502−509.

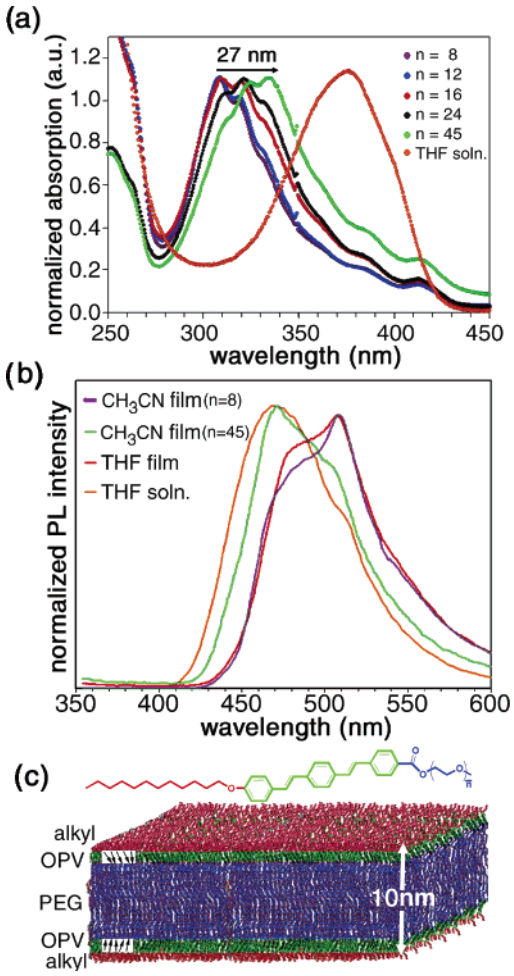

Figure 4. (a) Absorption and (b) photoluminescence of OPV amphiphile solutions and films of varying PEG length. All spectra are normalized to the same intensity to facilitate comparison of peak shape. (c) Bilayer packing model showing alkyl (red), OPV (green), and PEG (blue) layers. Inset arrows show approximate orientation of OPV transition dipole.

crystallization of longer PEGs should disrupt the smectic layers, thereby reducing OPV aggregation. Film PL depends on both solvent and PEG length, as observed by the PL emission maximum (λ_{PL}) of films spin-coated from CH_3CN, which shifts from 504 nm for **OPV-16** to 468 nm for longer amphiphiles (Figure 4b). In shorter OPV amphiphiles, aggregation and exciton coupling within the highly ordered OPV layer could explain the red-shifted λ_{PL}. At the same time, we propose that structural disorder of the OPV induced by crystallization of longer PEGs reduces aggregation and limits energy transfer between OPV chromophores, enhancing emission and leading to the observed PL spectra of OPV-45 films, which is almost identical to that of the molecule in dilute solution. It is at first counterintuitive that crystallization of one segment of the molecule (PEG) could increase disorder in another segment (OPV). However, this is consistent with the spectroscopic data and is reasonable considering the very different crystal structures of the two separate portions of the molecule, which likely prevent the amphiphile from adopting a packing geometry that is simultaneously favorable for both PEG and OPV. Thus, as the length of the PEG segment increases, its equilibrium structure dominates the overall behavior of the amphiphile, at the expense of the highly ordered OPV-driven structure present in shorter amphiphiles.

Table 3. Lyotropic LC Clearing Temperature and Lamellar Layer Spacing

solvent[a]	T_c (°C)	d_{100} (nm)[b]
H_2O	>100	11.0
DMSO	68	11.1
CH_3CN	55	11.3
DMF	52	13.1

[a] Mesophases formed with 40 wt % **OPV-45** in the listed solvent. [b] Layer spacing determined from first-order diffraction peak in SAXS.

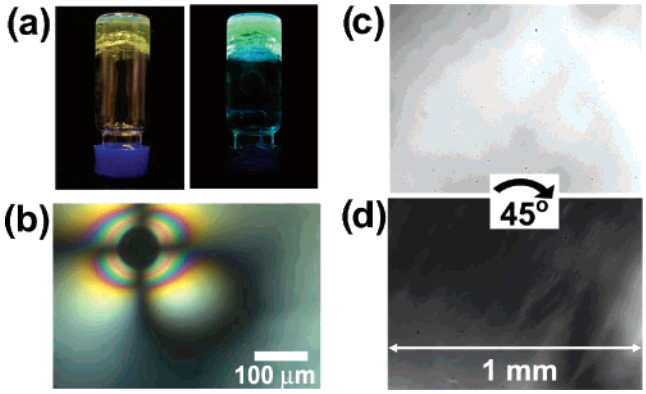

Figure 5. (a) Aqueous OPV amphiphile gel under visible (left) and 365 nm UV light (right). (b) Birefringent defect in homeotropically aligned aqueous LC. (c and d) Shear induced homogeneous alignment of aqueous LC. Switches uniformly from (c) bright to (d) dark on 45° rotation of crossed polarizers.

Aqueous Self-Assembly and Lyotropic Phases. OPV amphiphiles are soluble in most polar organic solvents and, for **OPV-24** or longer, are soluble in water as well. At high concentration (>30 wt %), they form lyotropic LC phases that likely consist of a solvent-swelled PEG layer and an aggregated OPV-alkyl layer. One expects, based on the Israelachvili packing model, that the bulky PEG chains of the longer amphiphiles would increase the curvature of the hydrophobic−hydrophilic interface, forming hexagonal or cubic mesophases.[27,28] Only lamellar structures are observed, however, possibly because OPV aggregation frustrates hydrophobic collapse, increasing the effective molecular cross section at the interface.

OPV-45 was used for the study of lyotropic LC gels since longer PEGs imparted better solubility and more promising PL behavior. Table 3 details results of DSC and SAXS on this amphiphile in solvents where mesophase behavior was observed.

The concentration used corresponds to a water−PEG ratio of 1.9:1 (w/w) or 4.6 water molecules per PEG repeat unit. This should result in full hydration of PEG, with hydrogen bonding saturated and nearly all water in the bound state.[29] As the solvent is largely immobilized, the mixture forms a highly viscous, transparent gel. Figure 5a is a photograph of the aqueous, self-supporting gel in an upturned vial, illuminated by either visible or UV light. The gels are strongly fluorescent despite the high concentration of OPV.

Figure 6 shows PL of aqueous OPV amphiphile solutions. At low concentrations, λ_{PL} is 473 nm, showing a small solvatochromic shift from the 468 nm peak in THF (Table 2).

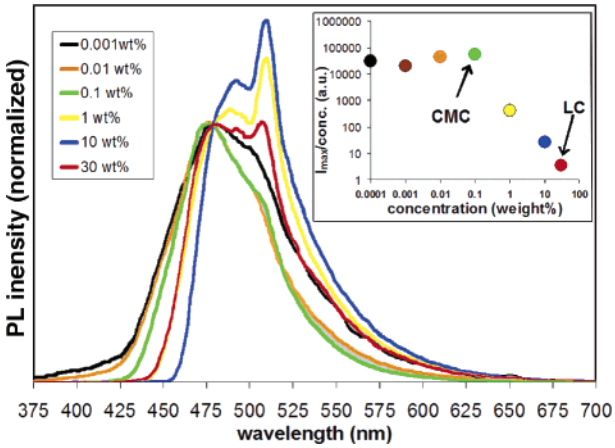

Figure 6. PL spectra for aqueous solutions of OPV amphiphiles at various concentrations (Ex = 375 nm). Spectra are normalized (at 475 nm) to facilitate comparison. Inset shows maximum intensity versus concentration, with CMC and LC transitions indicated.

PL intensity is directly proportional to concentration up to 0.1 wt %, beyond which a 30 nm red shift and exponential decrease in PL emission is observed, consistent with OPV aggregation above the critical micelle concentration (CMC) of the solution. A sharp shoulder appears at 505 nm, reaching a maximum at 10 wt % amphiphile, which could be vibronic in nature or due to J-aggregate formation. At 30 wt %, LC mesophase formation induces a surprising change in the shape of the PL spectrum. The peak at 505 nm diminishes, and the emission blue shifts toward that of dilute solutions, possibly due to confinement of the OPV within the layered LC structure, thus limiting intermolecular energy transfer.

Lamellar LC order was confirmed in the aqueous OPV amphiphile gel by POM and SAXS. When heated to 40 °C, the LC phase aligns homeotropically on glass (Figure 5b), likely due to strong interaction between PEG and the hydrophilic glass surface. The LC phase can also be oriented homogeneously through shear induced alignment (Figure 5c,d). Uniformly aligned regions several centimeters in diameter have been prepared, which is a significant improvement over thermotropic films where domain sizes are generally <100 μm (Figure 3). This suggests a facile route to align OPV amphiphile films by casting from a dilute aqueous solution. As water evaporates, the molecules undergo a transition through an LC phase, yielding ordered, aligned films on drying. SAXS confirmed that lamellar structure of the aqueous gel is retained on drying, though the layer spacing increases from 11 to 15 nm (Figure 7). This likely is due to rearrangement of the PEG chain, which typically adopts a 7/2 helical conformation (7 monomer repeat units per 2 turns) on drying with a pitch of 1.93 nm,[30] giving an expected length of 12.5 nm for **OPV-45**. Thus, the observed length is consistent with that of a lamellar packing model with a fully interdigitated PEG layer.

To confirm LC order is responsible for the novel photoluminescence of OPV amphiphile gels, we examined its temperature dependence. Aqueous gels remain in the LC phase up to the solvent's boiling point, thus, the temperature dependence of PL was determined for a 40 wt % gel of **OPV-45** in dimethyl sulfoxide (DMSO) instead of water. At this composi-

(27) Israelachvili, J. N. *Intermolecular and Surface Forces*, 2nd ed.; Academic Press: San Diego, CA, 1992.
(28) Kunieda, H.; Umizu, G.; Yamaguchi, Y. *J. Colloid Interface Sci.* **1999**, *218*, 88−96.
(29) (a) Borodin, O.; Bedrov, D.; Smith, G. D. *J. Phys. Chem. B* **2002**, *106*, 5194−5199. (b) Smith, G. D.; Bedrov, D.; Borodin, O. *Phys. Rev. Lett.* **2000**, *85*, 5583−5586.
(30) Yang, R.; Yang, X. R.; Evans, D. F.; Hendrickson, W. A.; Baker, J. *J. Phys. Chem.* **1990**, *94*, 6123−6125.

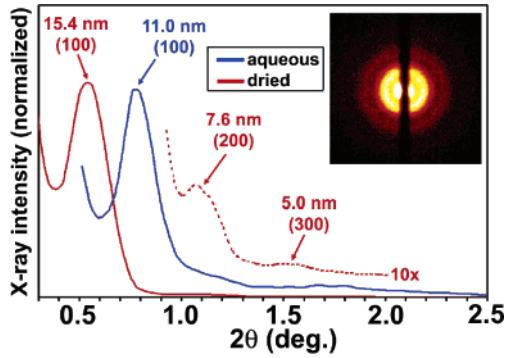

Figure 7. SAXS spectra of aqueous (blue) and dried (red) films of **OPV-45**, showing lamellar periodicity. Dashed line is magnified 10× to show higher-order peaks.

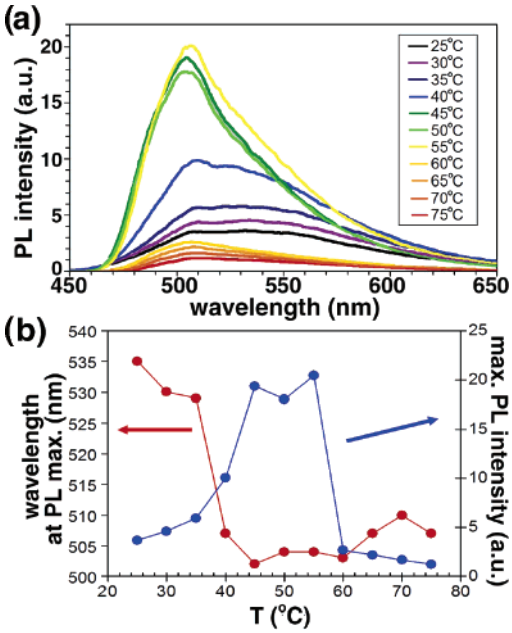

Figure 8. (a) PL spectra of 40 wt % DMSO gel at various temperatures (Ex = 375 nm). (b) Wavelength (red) and intensity of PL maximum versus temperature.

tion, the amphiphile crystallizes at room temperature, forms a lamellar LC between 38 and 68 °C, and an isotropic solution above. Figure 8 shows PL spectra for the DMSO gel at various temperatures. Strikingly, a 4-fold increase in PL intensity and a 25 nm blue shift occur on formation of the LC mesophase. On isotropization, PL intensity returns to its previous level. The transition is fully reversible, and similar results were obtained in other solvents, such as acetonitrile. While fluorescence varied significantly as a function of temperature, absorption did not, indicating that the observed behavior is not due to changes in scattering or absorption by the gel. Instead, it appears that photoluminescence is enhanced due to the ordered structure of the lyotropic liquid crystal, which could alter the OPV's aggregation state or limit exciton coupling and migration within the OPV sublayers of the lamellar structure. The ability to control the nanoscale structure and aggregation of OPV through amphiphilic self-assembly, as demonstrated in these systems, may prove useful in enhancing the performance of phenylene vinylene-based molecules for a variety of organic electronics applications.

Experimental Methods

General. Melting and mesophase transition temperatures were determined using a TA Instruments 2920 DSC/TGA. Ten milligram samples were placed in hermetically sealed Al pans and cycled three times at 5 °C min^{-1}. Transition temperatures were determined from the second heating cycle (all were fully reversible). Thermogravimetric analysis (TGA) showed an onset of decomposition at 190 °C on heating at 10 °C min^{-1} in air, which was well above the clearing temperature for all OPV amphiphiles investigated. Additionally, the stability of the molecule against thermal degradation was verified by NMR, which showed no change after heating the molecule to 180 °C for 4 h in air. Purity and polydispersity of the final product were determined using a Waters 2690 GPC in THF calibrated with polystyrene standards. A single peak was obtained for each amphiphile. POM was performed using a Leitz Laborlux 12POL polarizing microscope with a thermostatically controlled heating stage and a 35 mm film camera. Samples were sealed with a 75 μm spacer between pre-cleaned glass slides, heated to isotropization, and then cooled at 0.3 °C min^{-1} to obtain identifiable LC textures. SAXS spectra were collected on samples sealed in quartz capillary tubes using a Rigaku Cu Kα source at 33 kV and a 2D Bruker CCD detector calibrated with silver behenate. Wide-angle powder X-ray diffraction patterns were collected on a Scintag XDS2000 automated diffractometer with a Cu Kα source operating at 40 kV. UV−vis absorption was studied using a Cary 500 UV−vis−NIR spectrometer operating in double-beam mode. PL spectra were collected on a PC1 spectrofluorimeter in right angle geometry. Both instruments were fitted with heated, thermostatically controlled sample holders. For film measurements, 1 wt % solutions were spin-coated at 2000 rpm on quartz plates, yielding films 300 nm thick. For PL, film samples were placed at 45° to the detector. The excitation wavelength was chosen at the absorption maximum from UV−vis, but PL spectral shape was found to be relatively insensitive to excitation wavelength. Dilute solutions for fluorescence in THF were prepared by adjusting the concentration to an absorption of <0.1. For high-concentration solutions and LC gels, ultrashort (10 μm) path length quartz holders were used to allow adequate transparency. To ensure complete dissolution of the OPV amphiphile, lyotropic LC gels were prepared by dissolving the material at 10 wt % and then evaporating solvent to achieve the desired concentration. Samples were then heated in sealed vials to homogenize. HPLC grade solvents for LC experiments (THF, CH_3CH, and DMSO) were degassed prior to use, and DI water was purified using a Millipore filtration system.

The **OPV-8** amphiphile was synthesized by the following procedure. Other OPV-*n* amphiphiles were synthesized by a similar procedure beginning with longer poly(ethylene glycol) methyl ethers. Unless otherwise noted, all starting materials were obtained from commercial suppliers and used without further purification. 4-(Dimethylamino)-pyridinium-4-toluenesulfonate (DPTS) was prepared according to literature.[31] The ^{1}H NMR and ^{13}C NMR spectra were recorded on a Varian Unity 400 (400 MHz) or Unity 500 (500 MHz) spectrometer using the solvent proton signal as standard. Mass spectra were obtained on a Micromass Quattro II atmospheric pressure ionization (API) triple quadrupole mass spectrometer. Matrix-assisted laser desorption ionization-time-of-flight mass spectrometry (MALDI-TOF MS) was performed on an Applied Biosystems Voyager-DE Pro. Silica for flash chromatography was ICN Silitech 32-63 D 60 A.

Poly(ethylene glycol) Methyl Ether-4-bromomethyl Benzoate (1). α-Bromo-*p*-toluic acid (1.07 g, 5.00 mmol, 1.00 equiv), poly(ethylene glycol) methyl ether (M_w = 350 g/mol, 1.75 g, 5.00 mmol, 1.00 equiv), DPTS (1.56 g, 5.30 mmol, 1.06 equiv), and CH_2Cl_2 (150 mL) were all combined in a flask with a stirring bar. 1-(3-(Dimethylamino) propyl)-3-ethylcarbodiimide hydrochloride (1.44 g, 7.53 mmol, 1.50 equiv) was added, and the reaction mixture was stirred for 24 h at room temperature. The solution was washed with a 5% aqueous solution of citric acid and a saturated aqueous solution of NaCl. The organic layer was collected, dried with $MgSO_4$, filtered, and concentrated in vacuo.

(31) Granier, T.; Thomas, E. L.; Gagnon, D. R.; Karasz, F. E.; Lenz, R. W. *J. Polym. Sci., Part B: Polym. Phys.* **1986**, *24*, 2793−2804.

The product was subjected to a column chromatography using 5% MeOH/CH_2Cl_2 as the eluant to afford the product (2.2 g, 4.0 mmol, 80% yield). ^{1}H NMR (400 MHz, $CDCl_3$) δ: 8.06 (d, 2H, J = 7.9 Hz), 7.47 (d, 2H, J = 8.6 Hz), 4.63 (s, 2H), 4.50 (t, 2H, J = 4.9 Hz), 3.85 (t, 2H, J = 4.6 Hz), 3.67 (m, 24H), 3.39 (s, 3H). ^{13}C NMR (500 MHz, $CDCl_3$) δ: 166.0, 142.8, 130.4, 130.2, 129.0, 72.5, 71.9, 70.7, 70.6, 70.5, 70.2, 64.3, 61.6, 59.0, 32.3.

Poly(ethylene glycol) Methyl Ether-4-((diethylphosphono)methyl) Benzoate (2). Benzyl bromide **1** (1.0 g, 2.1 mmol, 1.0 equiv) and triethyl phosphite (0.72 mL, 4.2 mmol, 2.0 equiv) were placed in a flask with a magnetic stirring bar. A distillation apparatus was attached to collect ethyl bromide formed along with the reaction. The mixture was immersed in an oil bath and heated to 130 °C for 24 h. The reaction mixture was cooled, diluted with Et_2O, and washed with H_2O. The organic layer was dried with $MgSO_4$, filtered, and concentrated in vacuo. The resulting oil (1.29 g, 2.10 mmol, 100% yield) was used for the next Horner−Emmons reaction without further purification. ^{1}H NMR (400 MHz, $CDCl_3$) δ: 8.00 (d, 2H, J = 7.9 Hz), 7.37 (d, 2H, J = 7.3 Hz), 4.45 (t, 2H, J = 4.9 Hz), 4.01 (t, 2H, J = 6.7 Hz), 3.63 (m, 24H), 3.19 (d, 2H, J = 22.0 Hz).

Diethyl-4-cyanobenzyl Phosphonate (3). Compound **3** was prepared with α-bromo-*p*-tolunitrile (10 g, 51 mmol, 1.0 equiv) and triethyl phosphite (9.6 mL, 56 mmol, 1.1 equiv) via an Arbuzov condition similar to that of the reaction for **1** as a colorless oil (12.9 g, 51.0 mmol, 100% yield). ^{1}H NMR (400 MHz, $CDCl_3$) δ: 7.60 (d, 2H, J = 7.9 Hz), 7.41 (d, 2H, J = 7.9 Hz), 4.03 (m, 4H), 3.19 (d, 2H, J = 22.6 Hz), 1.25 (t, 6H, J = 7.0 Hz).

4-Dodecyloxybenzaldehyde (4). 4-Hydroxybenzaldehyde (5.0 g, 41 mmol, 1.0 equiv), potassium carbonate (8.5 g, 61 mmol, 1.5 equiv), dodecyl bromide (12.3 g, 49.2 mmol, 1.20 equiv), and 18-crown-6 (1.0 g, 4.1 mmol, 0.10 equiv) were placed in a flask with a magnetic stirring bar and a cooling column and were dissolved in 50 mL of acetone. The mixture was refluxed for 24 h. After the mixture was cooled, it was filtered and concentrated in vacuo. The crude product was subjected to a column chromatography using CH_2Cl_2 to afford the product as a pale yellow solid (10.3 g, 35.0 mmol, 87% yield). ^{1}H NMR (400 MHz, $CDCl_3$) δ: 9.85 (s, 1H), 7.83 (d, 2H, J = 8.6 Hz), 7.00 (d, 2H, J = 8.6 Hz), 4.05 (t, 2H, J = 6.4 Hz), 1.80 (m, 2H), 1.27 (m, 18H), 0.89 (t, 3H, J = 6.7 Hz). ^{13}C NMR (500 MHz, $CDCl_3$) δ: 191.0, 164.5, 132.2, 130.0, 115.0, 68.7, 32.2, 29.9, 29.8, 29.6, 29.3, 26.2, 22.9, 14.4. APCI-MS m/z 291.3 (M^+).

4-(2-(4-Dodecyloxyphenyl)-(*E*)-1-ethenyl)-1-benzonitrile (5). Lithium diisopropylamide mono(tetrahydrofuran) (LDA) (1.5 M solution in cyclohexane, 28.3 mL, 42.5 mmol, 1.20 equiv) and 50 mL of THF were placed in a dry flask using a magnetic stirring bar under N_2 and cooled to −78 °C. Phosphonate **3** (9.0 g, 35 mmol, 1.0 equiv), dissolved in 50 mL of THF, was added dropwise into the precooled solution with a dropping funnel. The reaction mixture was placed in a 0 °C ice bath, and aldehyde **4** (10.3 g, 35.4 mmol, 1.00 equiv), dissolved in 50 mL of THF solution, was added dropwise into the mixture. The reaction mixture was stirred overnight at room temperature and quenched by adding an aqueous solution of acetic acid. THF was removed by evaporation, and a yellowish-white solid that precipitated out in the water layer was collected by filtration. The crude product was subjected to a column chromatography using CH_2Cl_2 to afford the product as a pale yellow solid (10.9 g, 28.0 mmol, 79% yield). ^{1}H NMR (400 MHz, $CDCl_3$) δ: 7.61 (d, 2H, J = 8.5 Hz), 7.54 (d, 2H, J = 7.9 Hz), 7.46 (d, 2H, J = 8.5 Hz), 7.16 (d, 1H, J = 16.5 Hz), 6.94 (d, 1H, J = 16.5 Hz), 6.90 (d, 2H, J = 8.6 Hz), 3.98 (t, 2H, J = 6.4 Hz), 1.79 (m, 2H), 1.45 (m, 2H), 1.26 (m, 16H), 0.88 (t, 3H, J = 6.7 Hz). ^{13}C NMR (500 MHz, $CDCl_3$) δ: 160.0, 142.5, 132.7, 132.3, 128.5, 127.3, 126.8, 124.6, 119.4, 115.1, 114.8, 68.4, 32.2, 29.9, 29.7, 29.6, 29.5, 26.3, 22.9, 14.4. APCI-MS m/z 390.5 (M^+).

4-(2-(4-Dodecyloxyphenyl)-(*E*)-1-ethenyl)-1-benzaldehyde (6). Nitrile **5** (10.6 g, 36.8 mmol, 1.00 equiv) was dissolved in 500 mL of Et_2O and cooled to 0 °C. Diisobutylaluminum hydride (1.0 M solution in hexane, 55.2 mL, 55.2 mmol, 1.50 equiv) was added dropwise into the solution using a dropping funnel. The solution was stirred at 0 °C for 20 min and poured into 10% AcOH/H_2O (500 mL). The ether layer was evaporated in vacuo, and a yellow solid precipitated out in the water layer and was collected by filtration. The crude product was subjected to a column chromatography using CH_2Cl_2 to afford the product as a yellow solid (8.4 g, 21 mmol, 58% yield). ^{1}H NMR (400 MHz, $CDCl_3$) δ: 9.98 (s, 1H), 7.85 (d, 2H, J = 7.9 Hz), 7.62 (d, 2H, J = 7.9 Hz), 7.48 (d, 2H, J = 8.6 Hz), 7.22 (d, 1H, J = 16.5 Hz), 7.00 (d, 1H, J = 16.5 Hz), 6.91 (d, 2H, J = 8.6 Hz), 3.98 (t, 2H, J = 6.7 Hz), 1.79 (m, 2H), 1.45 (m, 2H), 1.26 (m, 16H), 0.88 (t, 3H, J = 6.7 Hz). ^{13}C NMR (500 MHz, $CDCl_3$) δ: 191.9, 159.9, 144.2, 135.2, 132.1, 130.5, 129.3, 128.5, 126.8, 125.2, 115.1, 68.4, 32.2, 29.9, 29.7, 29.6, 29.5, 26.3, 22.9, 14.4. APCI-MS m/z 393.4 (M^+).

(Poly(ethylene glycol) Methyl Ether)-4-(2-(4-(2-(4-dodecyloxyphenyl)-(*E*)-1-ethenyl)phenyl)-(*E*)-1-ethenyl)-1-benzoate (OPV-8). OPV-8 amphiphile was prepared with aldehyde **6** (0.36 g, 0.92 mmol, 1.0 equiv), phosphonate **2** (0.5 g, 0.9 mmol, 1 equiv), and LDA (1.5 M solution in cyclohexane, 0.74 mL, 1.1 mmol, 1.2 equiv) via the Horner−Emmons condition similar to that of the reaction for compound **5**. The crude product was extracted with CH_2Cl_2 and subjected to a column chromatography using 5% MeOH/CH_2Cl_2 to afford the product as a yellow solid (0.56 g, 0.66 mmol, 72% yield). M_w/M_n = 1.01. MALDI-TOF MS m/z 900.2 ($M + Na^+$). ^{1}H NMR (400 MHz, $CDCl_3$) δ: 8.05 (d, 2H, J = 8.6 Hz), 7.58 (d, 2H, J = 8.6 Hz), 7.52 (d, 4H, J = 3.1 Hz), 7.46 (d, 2H, J = 8.5 Hz), 7.23 (d, 1H, J = 16.5 Hz), 7.14 (d, 1H, J = 16.5 Hz), 7.11 (d, 1H, J = 16.5 Hz), 6.98 (d, 1H, J = 16.5 Hz), 6.91 (d, 2H, J = 8.6 Hz), 4.45 (t, 2H, J = 4.5 Hz), 3.99 (t, 2H, J = 6.7 Hz), 3.85 (t, 2H, J = 4.6 Hz), 3.65 (m, 24H), 1.79 (m, 2H), 1.45 (m, 2H), 1.27 (m, 16H), 0.89 (t, 3H, J = 6.7 Hz). ^{13}C NMR (500 MHz, $CDCl_3$) δ: 166.5, 159.3, 142.2, 138.0, 135.8, 131.1, 130.4, 130.0, 129.0, 128.9, 128.0, 127.4, 127.3, 126.8, 126.5, 126.0, 114.9, 72.1, 70.9, 70.8, 69.5, 68.3, 64.3, 59.2, 32.1, 29.9, 29.8, 29.6, 29.6, 29.5, 26.3, 22.9, 14.4.

Conclusions

We have reported on a novel series of amphiphilic molecules consisting of an OPV trimer end-substituted asymmetrically with a hydrophobic alkyl chain and a hydrophilic ethylene glycol chain, which self-assemble forming both thermotropic and lyotropic liquid crystalline mesophases. By varying the length of the ethylene glycol block, one can change the structure and solubility of the amphiphile, altering its optoelectronic properties. Photoluminescence from films of the amphiphile with the longest hydrophilic chain resembles that of molecules in dilute solution, indicating that self-assembly dramatically alters the aggregation behavior of the OPV chromophore. The layered LC phase appears to inhibit OPV aggregation and reduce exciton migration, leading to enhanced and blue-shifted photoluminescence. Formation of ordered OPV amphiphile mesophases provides a facile route to prepare nanostructured films in which the structural and optical properties are controlled to a degree not possible with soluble PPV polymers or other substituted OPVs.

Acknowledgment. This work made use of the Keck Biophysics Facility, the Jerome B. Cohen X-ray Diffraction Facility, and the Analytical Services Laboratory at Northwestern University. J.F.H. is supported by an NDSEG fellowship and a Northwestern Presidential Fellowship. The work was supported by the U.S. Department of Energy under Award DE-FG02-00ER54810.

Supporting Information Available: Differential scanning calorimetry, MALDI-TOF MS, and additional photoluminescence spectra of OPV amphiphiles. This material is available free of charge via the Internet at http://pubs.acs.org.

JA047210M